2022

Compressor Speed, Expansion Valve Opening and Refrigerant Charge Influences on the Propane Unit Design

Zvonimir Jankovic

Branimir Pavkovic

Jaime Sieres

Marija Zivic

Compressor Speed, Expansion Valve Opening and Refrigerant Charge Influences on the Propane Unit Design

Zvonimir JANKOVIC [1,4]*, Branimir PAVKOVIC [2], Jaime SIERES[3], Marija ZIVIC[1]

[1] Department of Energetics, Mechanical Engineering Faculty in Slavonski Brod, University of Slavonski Brod, Trg Ivane Brlić-Mažuranić 2, 35000 Slavonski Brod, Croatia
zjankovic@unisb.hr

[2] Department of Thermodynamics and Energy Engineering, Faculty of Engineering, University of Rijeka, Vukovarska 58, 51000 Rijeka, Croatia
branimir.pavkovic@riteh.hr

[3] Área de Máquinas y Motores Térmicos, Escuela de Ingeniería Industrial, University of Vigo, Campus Lagoas-Marcosende 9, 36310 Vigo, Spain
jsieres@uvigo.es

[4] WSL Refrigeration d.o.o., Sneberska c. 111B, 1260 Ljubljana – Polje, Slovenia
zvonimir.jankovic@wsl-refrigeration.com

*corresponding author

ABSTRACT

This research involves the development of a computational tool for the design of a vapor-compression liquid-cooled chiller unit. It is suitable for the analysis of the unit design. The calculation tool was developed as a steady-state model with the following boundary conditions: compressor design and displacement, expansion valve nominal capacity, inlet temperatures and flow rates of the two secondary heat transfer fluids in the evaporator and condenser. The tool is designed to provide a better analysis of the thermodynamic process of compression refrigeration systems than using estimated condensing and evaporating temperatures for process analysis. The mathematical model is able to compare the application of different refrigerants and components of the refrigeration system. The model was developed as a numerical tool using the Engineering Equation Solver (EES), which includes a detailed model of the compression process and energy balance of the compressor, a model of the expansion valve to predict valve opening, and full correlations of heat transfer and pressure losses in all heat exchangers of the refrigeration cycle. The simulation model is validated with specific steady state experimental tests performed on a propane refrigeration machine. The case study is conducted to analyze the effects of refrigerant charge, subcooling level, and expansion valve openings on the performance of the propane unit.

1. INTRODUCTION

The European Regulation on Certain Fluorinated Greenhouse Gases 517/2014 (EU) has had a significant impact on scientific research in recent years. This regulation leads to the retrofit or conversion of refrigerators and heat pumps to alternative refrigerants, which generally have a low impact on the atmosphere, leading to the increasing use of natural refrigerants as a base. Of this group, propane refrigerant (R290) is one of the best current options for residential and commercial refrigerators and freezers in the refrigeration sector, and also for chillers and heat pumps in the air conditioning sector. This refrigerant is highly flammable. For this reason, directives 2009/125/ EC (Ecodesign and Energy Labelling Directive) and 2006/42/ EC (Machinery Directive) control the amount of flammable refrigerant in the refrigeration circuit during the design of the equipment. This opens the possibility that the research on the optimal refrigerant charge and the selection of components is applicable and useful for the design of the equipment. R290, with its very good thermodynamic properties and very low global warming potential (GWP=3), is becoming increasingly common in new refrigeration equipment. In the design of propane refrigeration units, the liquid receiver is often omitted or indirectly not allowed because of the limited refrigerant charge. Therefore, in the design of refrigeration units, the selection of components, the operating frequency of the compressor and the opening of the expansion valve (or the length and diameter of the capillary tube) must correlate with the optimal refrigerant charge to obtain good working conditions. The example of the propane chiller is used to present this methodology for the design of propane chillers, which is also the objective of this article.

2. MATHEMATICAL MODEL

A mathematical model is developed for each component - the component models. Based on the component models, the calculation model for the thermodynamic simulation of the propane unit, in this case the chiller, is unified. Simulated components: semi-hermetic reciprocating compressor; electronic or thermostatic expansion valve; BPHE evaporator; BPHE condenser; BPHE liquid-vapour heat exchanger. All mathematical models take into account specific data and dimensions of the components with the aim of predicting the actual operating conditions of the chiller. Heat transfer between the environment and the heat exchangers is neglected; pressure losses in the refrigerant lines between the main components are neglected. The simulation tool was programmed with the Engineering Equation Solver (EES).

2.1 Compressor

Mathematical mode of semi-hermetic reciprocating compressor was separated in two parts:

- The calculation of the refrigerant mass flow (main correlations presented in the Table 1);
- Energy balance of compressor.

The calculation of the refrigerant mass flow is based on the effective displacement of the compressor. It is necessary to determine the cylinder displacement of the compressor, the number of revolutions per minute and the volumetric efficiency of the compressor (η_1, η_2, η_3, η_4):

$$\dot{V}_{ef} = V_{piston} \cdot \dot{N}_{rot} \cdot \eta_{vol} \rightarrow \dot{m}_{ref} = \dot{V}_{ef} \cdot \rho_{[1]} \quad (1)$$

The volumetric efficiency of a compressor indicates by how much the effective displacement of the compressor is less than the theoretical volumetric flow rate of the compressor, calculated according to the following equation:

$$\eta_{vol} = \eta_1 \cdot \eta_2 \cdot \eta_3 \cdot \eta_4 \quad (2)$$

This calculation includes: the influence of clearance volume η_1, the pressure drop of the refrigerant between the compressor inlet and the cylinder η_2, the heating of the refrigerant from the compressor inlet to the inlet of the cylinder η_3 and the refrigerant leakage η_4.

Table 1: Correlations for modeling the compression process

Influence of clearance volume

$$\eta_1 = 1 - \varepsilon_0 \cdot \left(\left(\frac{p_{cond}}{p_{evap}} \right)^{\left(\frac{1}{n}\right)} - 1 \right); \varepsilon_0 = \frac{V_0}{V_{piston}}; n = \frac{\log\left(p_{[1]} / p_{[2]} \right)}{\log\left(v_{[2]} / v_{[1]} \right)}$$

Influence of pressure drop on the suction valve (SV) and discharge valve (DV) of the compressor (Boeswirth and Milanova ,1998)

$$\eta_2 = 1 - \frac{\Delta p_{SV}}{p_{[1]}}; \Delta p_{SV} = p_{[1]} \cdot \Delta\eta_{SV}; \Delta\eta_{SV} = \left(1 - \varepsilon_0 \cdot \left(\left(p_{cond} / p_{evap} \right)^{\left(\gamma/n\right)} - 1 \right) \right) \cdot \frac{w_{loss,SV}}{c_{p,ref,cyl,inlet} \cdot T_{ref,cyl,inlet}}$$

$$\dot{W}_{loss,SV} = 3.41 \cdot \frac{\left(V_{piston} \cdot \dot{N}_{rot} \right)^3 \cdot \rho_{ref,cyl,inlet} \cdot \left(\eta_3 \cdot \eta_4 \right)^2}{N_{SV} \cdot A_{ef}^2} \cdot \left(1 - \varepsilon_0 \right) \cdot \left(1 + 0.85 \cdot \left(PF - 1 \right) \right) \cdot \left(1 - \left(0.7 \cdot \eta_3 \cdot \eta_4 \cdot Ma_m \right)^2 \right)$$

Mach number (Ma_m)

$$Ma_m = \frac{A_{piston}}{A_{ef}} \cdot 2 \cdot \Delta z_{piston} \cdot \frac{\dot{N}_{rot}}{\sqrt{\frac{\kappa \cdot p_{ref,cyl,inlet}}{\rho_{ref,cyl,inlet}}}}$$

Discharge valve (DV) (included in the energy balance):

$$\dot{W}_{loss,DV} = 3.41 \cdot \left(\frac{\left(V_{piston} \cdot \dot{N}_{rot} \right)^3 \cdot \rho_{ref,cyl,inlet} \cdot \eta_3 \cdot \eta_4 \cdot \left(p_{cond} / p_{evap} \right)^{\left(\frac{1}{n}\right)}}{N_{DV} \cdot A_{ef}^2} \right) \cdot \left(\frac{1}{\left(p_{cond} / p_{evap} \right)} - 0.065 \right) \cdot \left(1 - 1.76 \cdot \varepsilon_0 \right) \cdot \left(1 + 1.75 \cdot \left(n - 1 \right) \right) \cdot PF$$

Influence of the heating of the refrigerant

$$\eta_3 = \frac{T_{[1]}}{T_{ref,cyl,inlet}}$$

The factor *PF* (pocket factor), which defines the design characteristics of the suction valve is between a value of 1.5 and 2 (Bauer, 1988). Refrigerant leakage is considered negligible in this analysis, therefore η_4=1.
The energy balance of the semi-hermetic reciprocating compressor, shown in the next figure, is programmed with the following equations:

$$\dot{W}_{el} = \dot{m}_{ref} \cdot \left(h_{[2]} - h_{[1]} \right) + \dot{Q}_{amb} \tag{3}$$

$$\dot{Q}_{SC} = \dot{Q}_{loss} + \dot{Q}_{DC} - \dot{Q}_{amb} \tag{4}$$

$$\dot{W}_{ref,in} = \dot{W}_{meh} \cdot \eta_{meh} = \dot{m}_{ref} \cdot \left(h_{cyl,inlet} - h_{cyl,outlet} \right)_{ref} + \dot{W}_{loss,SV} + \dot{W}_{loss,DV} \tag{5}$$

Heat transfer rate caused by electrical (el) and mechanical (mech) losses of the compressor:

$$\dot{Q}_{loss} = \left(1 - \eta_{el} \cdot \eta_{mech} \right) \cdot \dot{W}_{el} \tag{6}$$

Heat transfer rate to compressor's surroundings:

$$\dot{Q}_{amb} = \varepsilon_{\dot{Q},amb} \left(1 - \eta_{el} \cdot \eta_{mech} \right) \cdot \dot{W}_{el} \rightarrow \left(\varepsilon_{\dot{Q},amb} = 0.9 \right) \tag{7}$$

The mechanical losses for this family of compressors can be assumed between 5% and 10% (Scarpa ,2012).
The electrical efficiency η_{el} for semi-hermetic reciprocating compressors is defined according to the model of Scarpa (2012), which considers the relationship between the power of the electric motor and the actual electrical power (required to operate the compressor), as well as the frequency of the electric motor. The relationship between the actual electric power and the frequency of the electric motor are modeled according to Scarpa (2012) what can be applied to typical electric motors of this group of compressors. The indicated efficiency of a semi-hermetic reciprocating compressor is defined according to Hengel (2016), which is generally applicable to reciprocating compressors. The relationships between the electrical efficiency, the indicated efficiency and the total efficiency for the simulation of a semi-hermetic reciprocating compressor are shown in the next figure and with the following equation:

$$\eta_{ov} = \eta_{in} \cdot \eta_{el} \cdot \eta_{mech} \tag{8}$$

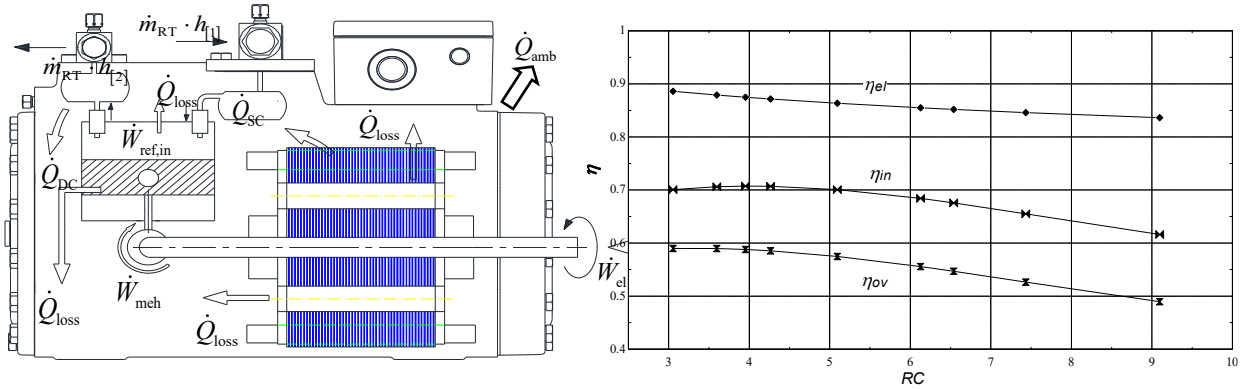

Figure 1: Energy balance and efficiencies of the semi-hermetic reciprocating compressor

2.2 Electronic expansion valve

The mathematical model of the electronic expansion valve (EEV) was developed to be used for various vapour compression applications and cooling capacities. The EEV increases or decreases its orifice area to allow a refrigerant mass flow that provides the best use of the evaporator heat exchange area required to maintain the required refrigerant superheat.
The models of all parts of the refrigeration unit use the refrigerant mass flow rate defined by the compressor model that must converge through the expansion valve, resulting in the required flow area and percentage of expansion valve opening required, which provides information on the required valve capacity and valve opening. Based on this, dimensionless correlations were developed to calculate the valve opening as a function of the ratio between the actual flow area A_{EV} and the maximum flow area $A_{EV,max.}$, of the valve. The dimensionless correlations are shown in the diagram of next figure for different operating frequencies of the compressor or different refrigerant mass flow rates. The same correlations may be used for EEV and standard mechanical expansion valves (EV).

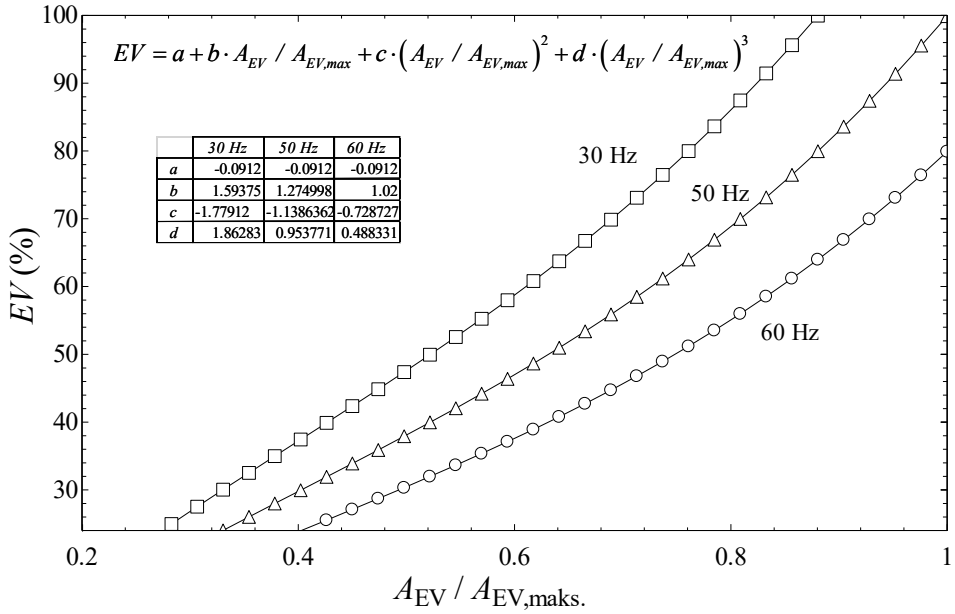

	30 Hz	50 Hz	60 Hz
a	-0.0912	-0.0912	-0.0912
b	1.59375	1.274998	1.02
c	-1.77912	-1.1386362	-0.728727
d	1.86283	0.953771	0.488331

Figure 2: Correlation of EV opening in the function of the ratio of required and maximal flow area

To calculate the mass flow through the expansion valve, we need to calculate the flow factor C_{EV}, the flow area A_{EV}, the expansion factor Y_{EV}, the density of the liquid phase of the refrigerant $\rho_{[3]}$ at the inlet of the expansion valve, and the pressure difference that the valve must relieve Δp_{EV}:

$$\dot{m}_{ref} = C_{EV} \cdot A_{EV} \cdot Y_{EV} \cdot \sqrt{\left(2 \cdot \rho_{[4]} \cdot \Delta p_{EV}\right)} \tag{10}$$

The expansion factor Y_{EV} includes the change in refrigerant density flowing from the valve inlet to the inlet in the area of reduced pressure, related to the change in flow area as well as the pressure drop across the valve (Table 2). The expansion factor is influenced by the ratio between the diameters of the needle and the valve opening, the ratio of the pressure drops, the ratio of the specific heat capacities and the flow characteristics.

Table 2: Correlations for expansion factor calculation (American National Standards Institute, 2007)

$Y_{EV} = 1 - \frac{x_{EV}}{3 \cdot F_k \cdot x_T}$; $F_k = \frac{\left(c_p / c_v\right)}{1,4}$
$x_{EV} = \frac{\Delta p_{EV}}{p_{[3]}} = \frac{p_{cond} - p_{evap}}{p_{[3]}}$; $x_{EV} = F_k \cdot x_T \rightarrow$ "chocked flow" ($Y_{EV} = 2/3$)
x_{EV} pressure differential ratio of expansion valve x_T pressure differential ratio for heat influence of fluid (in this case R290)

Calculation of the flow factor is based on Buckingham π-theorem W. Li (2013). Flow factor C_{EV} is in the function of subcooling temperature and valve opening.

$$C_{EV} = e_1 \cdot \pi_1^{e_2} \cdot \pi_2^{e_3} \tag{11}$$

where π_1 defines the valve opening, and π_2 presents relation between superheat degree and critical temperature of refrigerant as follows:

$$\pi_2 = \Delta \vartheta_{sub} / \vartheta_{ref,critical} \tag{12}$$

The geometry input data of EV is based on the research papers of W. Li (2013), Y. Qifang (2007) and Z. Chuan (2006), while empirical coefficients for calculating the flow factor were determined experimentally in the named researches.

The idea of the described approach in modelling the EEV or standard EV is to allow the application of the model to the different refrigeration units with similar expansion valves and different performances. Mathematical model of EV defines the openings (area ratios). By reducing refrigerant mass flow rate, the maximum area ratio can actually be achieved and the valve never needs to be 100% open, by increasing refrigerant mass flow rate, the valve achieves 100% opening while the maximum area ratio is not possible – *this possibility is the aim of the EV model.*

2.3 Plate heat exchangers

The process of evaporation heat transfer is observed in two parts: heat transfer in the boiling zone and heat transfer in the superheated zone. Heat transfer correlations from well-known authors are used and tested. For the condensation process, the refrigerant side surface temperature of the condenser was always lower than the dew point temperature of the refrigerant. Therefore, only two zones (condensation and liquid subcooling) are considered in the analysis. LVHE has single-phase flows. The heat transfer correlations are shown in the next table. Energy balances in the BPHE are described in author's previous works (Janković and Sieres 2016)

Table 3: Heat transfer correlations for BPHE

Evaporation heat transfer correlations in the BPHE; Amalfi (2016)
$\alpha_{(nb+sp)} = 18.495 \cdot \frac{\lambda_{kap}}{d_{hyd,evap}} \cdot \left(\frac{\beta_{evap}}{\beta_{evap,max}}\right)^{0.248} \cdot \left(\frac{x_{[4]} \cdot \dot{M}_{ref,evap} \cdot d_{hyd,evap}}{\upsilon_{vapor}}\right)^{0.135} \cdot \left(\frac{\dot{M}_{ref,evap} \cdot d_{ref,evap}}{\upsilon_{vapor}}\right)^{0.351} \cdot \left(\frac{\rho_{liquid}}{\rho_{vapor}}\right)^{0.223} \cdot \mathrm{Bd}_{evap}^{0.235} \cdot \mathrm{Bo}_{evap}^{0.198}$
Boiling number ($\mathrm{Bo_{isp}}$), *and Bond number* ($\mathrm{Bd_{evap}}$); *Reynolds* (Re) *and Prandtl* (Pr) *numbers*
$\mathrm{Bo}_{evap} = \frac{q_{(nb+sp)}}{\dot{M}_{ref,evap} \cdot \Delta r_{evap}}$; $\mathrm{Bd}_{evap} = \left(\rho_{liquid} - \rho_{vapor}\right) \cdot g \cdot \frac{d_{hyd,evap}^2}{\sigma_T}$; $\Delta r_{evap} = h_{x=1} - h_{x=x_{[4]}}$; β – plate angle; σ_T – surface tension;
Condensation heat transfer correlation, BPHE; Nusselt (1919) $\mathrm{Re_{cond,ref}} \leq 1600$
$\alpha_{cond,ref} = 0.943 \cdot \left[\rho_{liquid} \cdot g \cdot \Delta h_{liquid\text{-}vapor} \cdot \frac{\left(\rho_{liquid} - \rho_{vapor}\right) \cdot \lambda_{liquid}^3}{\upsilon_{liquid} \cdot H_{cond,plate} \cdot \left(T_{cond} - T_{cond,plate}\right)}\right]^{0.25}$
Condensation heat transfer correlation, BPHE; Longo (2015) $\mathrm{Re_{cond,ref}} > 1600$
$\alpha_{cond,ref} = \alpha_{cond,ref,2ph} + F_C \cdot \left(\alpha_{cond,ref,1ph} + \frac{c_{p,ref,liquid} \cdot q_{cond}}{\Delta r_{cond}}\right)$
$\alpha_{cond,ref,2ph} = 1.875 \cdot \phi_C \cdot \frac{\lambda_{liqid}}{\mathrm{d}_{hyd,cond}} \cdot \mathrm{Re}_{cond,ref,ekv}^{0,445} \cdot \mathrm{Pr}_{cond,ref,liquid}^{(1/3)}$; $\phi_C = 1$ ("flat surface") ; $F_C = \frac{T_{[3]} - T_{cond}}{T_{cond} - T_{cond,plate}}$
One phase heat transfer inside BPHE, Thonon (1995) and Longo (2015)
$\alpha_{ref,1ph} = 0.2267 \cdot \frac{\lambda_{vapor}}{\mathrm{d}_{hyd}} \cdot \mathrm{Re}_{ref,vapor}^{0.631} \cdot \mathrm{Pr}_{ref,vapor}^{(1/3)}$
$\alpha_{liquid,1ph} = 0.2946 \cdot \frac{\lambda_{fluid}}{\mathrm{d}_{hid}} \cdot \mathrm{Re}_{fluid}^{0,7} \cdot \mathrm{Pr}_{fluid}^{(1/3)}$

The pressure drop (Δp_t) is calculated for all BPHE from the pressure drops due to influence of friction (Δp_f), momentum (Δp_a), gravity (Δp_g) and pressure drops in manifolds and ports (Δp_c). The pressure drop equations (including the correlations from Table 4) for the 2-phase and 1-phase heat exchangers are as follows:

$$\Delta p_{2ph,t} = \Delta p_{2ph,f} + \Delta p_{2ph,c} + \Delta p_{2ph,a} + \Delta p_{2ph,g} \tag{13}$$

$$\Delta p_{1ph,t} = \Delta p_{1ph,f} + \Delta p_{1ph,c} + \Delta p_{1ph,g} \tag{14}$$

Table 4: Pressure drop correlations for BPHE

Collier and Thome (1996)
$\Delta p_a = \dot{M}_{ref}^2 \cdot \left(v_{vapor} - v_{liquid}\right) \cdot \Delta x$
$\Delta p_g = g \cdot \rho_{R290} \cdot H$
Shah and Focke (1988); Longo and Gasparella (2007) *Longo (2008); Experimentally obtained for 1-phase flow refrigerant*
$\Delta p_c = \frac{1{,}5 \cdot \dot{M}_{RT}^2}{2 \cdot \bar{\rho}_{RT}}$; $\Delta p_{evap,f} = 1553 \cdot \frac{\dot{M}_{ref,evap}^2}{2 \cdot \bar{\rho}_{evap,ref}}$
$\Delta p_{cond,f} = 2050 \cdot \frac{\dot{M}_{ref,evap}^2}{2 \cdot \bar{\rho}_{cond,ref}}$; $\Delta p_{1ph,f} = 100 \cdot \frac{\dot{M}_{ref}^2}{2 \cdot \bar{\rho}_{ref}}$

2.4 Calculation of optimal refrigerant charge

The mathematical model described previously can be extended to include a simplified calculation of the refrigerant charge and obtain optimal working conditions for the propane system (in this case, the chiller). The mathematical model of refrigerant charge was developed based on Vjacheslav (2001).

To include the complete refrigerant mass charge M (kg) in this model, the refrigerant mass in each component and phase of the refrigeration system must be calculated:

$$M_{\text{mass,R290}} = M_{\text{comp}} + M_{\text{pipe,suction line}} + M_{\text{pipe,high pressure}} + M_{\text{pipe,liquid}} + M_{\text{LVHX,liquid}} + M_{\text{LVHX,vapour}} + M_{\text{evap}} + M_{\text{cond}} \quad (15)$$

The total amount of mass within refrigeration system can be approximated by (Vjacheslav, 2001):

$$M_{\text{mass,R290}} = M_{\text{evap}} + M_{\text{cond}} = \left(M_{\text{2ph}} + M_{\text{sup}}\right)_{\text{evap}} + \left(M_{\text{2ph}} + M_{\text{sub}}\right)_{\text{cond}}; \quad (16)$$

For a system without a liquid receiver, increasing the refrigerant mass leads to refrigerant accumulation in the condenser and, consequently, higher values of the degree of subcooling. If the refrigerant charge changes so does the surface area of the condenser used for the subcooling process. If it is assumed that all additional subcooled refrigerant charge will be accumulated in the condenser, then:

$$\Delta M_{\text{mass,R290}} = \frac{d_{\text{hyd,cond}}}{4} \cdot \Delta A_{\text{cond,R290}} \cdot \rho_{\text{cond,L}}; \quad (17)$$

An increase in the refrigerant mass by $\Delta M_{\text{mass,R290}}$ produces an increase of $T_{\text{cond},\Delta}$ of the condensation temperature. The relationship between refrigerant charge and condensation temperature changes are calculated from the following equation (Vjacheslav, 2001):

$$\frac{T_{\text{cond},\Delta} - T_{\text{fluid}}}{T_{\text{cond}} - T_{\text{fluid}}} = \frac{1}{\left(1 - \dfrac{\Delta A_{\text{cond,R290}}}{A_{\text{cond,sub}}}\right)} \rightarrow T_{\text{cond},\Delta} \rightarrow f\left(\Delta M_{\text{mass,R290}}\right). \quad (19)$$

3. TESTED PROPANE UNIT – MODEL VALIDATION

The model has been implemented and validated to simulate the performance of a propane chiller. Figure 3 shows a schematic representation of the chiller and a typical working cycle on a *p-h* diagram.

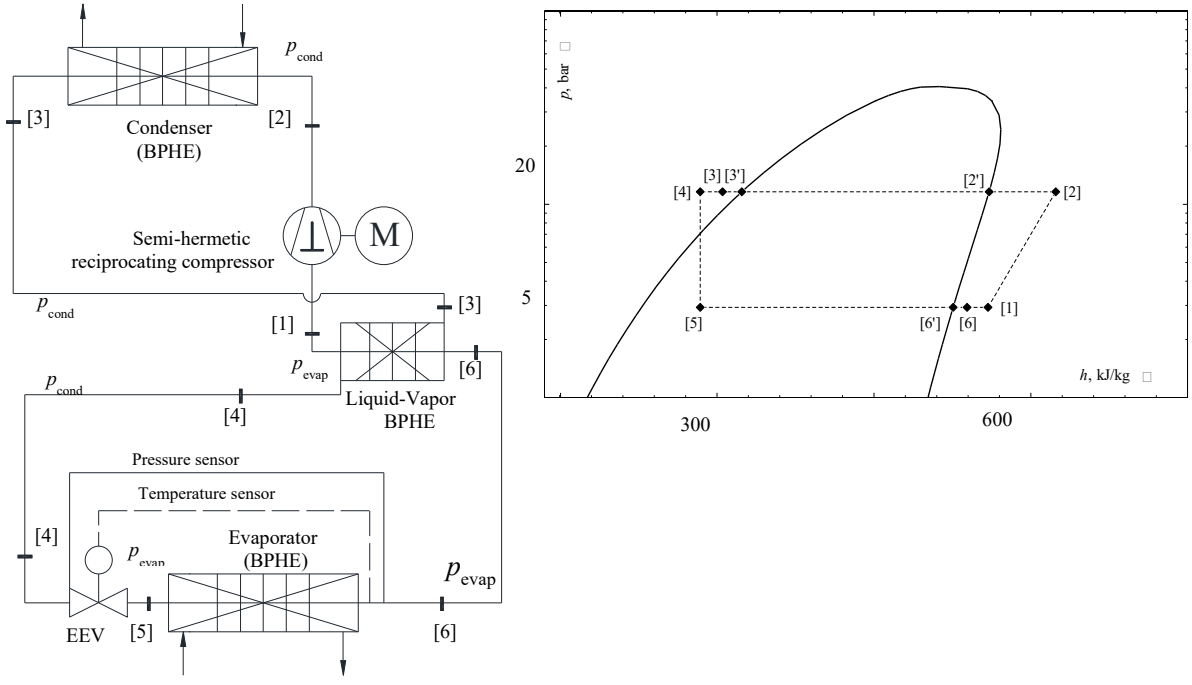

Figure 3: Schematic of tested propane chiller and main points (log *p*, *h* – diagram)

The semi-hermetic reciprocating compressor has 2 cylinders, giving a theoretical volumetric flow rate of 16.4 m^3/h at an operating frequency of 50 Hz. The BPHE evaporator has a plate width of 119 mm, a plate height of 329 mm, a channel width (distance between plates) of 2 mm and a plate thickness of 0.2 mm. The number of effective plates is 38, with 20 channels for water and 19 channels for refrigerant (R290). The BPHE condenser has a plate width of 124 mm, a plate height of 479 mm, a channel width (distance between plates) of 2 mm, and a plate thickness of 0.2 mm. The number of effective plates is 34, with 18 channels for EGV and 17 channels for refrigerant (R290). The

internal liquid - vapor BPHE has a plate width of 119 mm, a plate height of 234 mm, a channel width (distance between plates) of 2 mm, and a plate thickness of 0.2 mm. The number of effective plates is 6, with 3 channels for liquid refrigerant and 4 channels for vapor refrigerant. EEV has a nominal power of 12.4 kW for the refrigerant R407C, 13.7 kW for R410A, and 9.1 kW for R134a, with a condensing temperature of 38°C and an evaporating temperature of 4°C and subcooling of 1°C. At the above boundary conditions, the nominal cooling capacity of EEV is 12 kW for R290 refrigerant. EEV is controlled by a separate microprocessor (driver) programmed so that under all operating conditions the degree of superheat at the evaporator outlet is 6°C. Measuring equipment is presented in the next table.

Table 5: Measuring and controlling equipment of propane chiller

Measured value	**Measuring equipment**	**Measuring area**	**Accuracy/Characteristic**
Water temperatures	NTC sensor	Od -40°C do +105°C	R=27.3 kΩ @=0°C R=12.1 kΩ @=20°C
Temperature of R290 at evaporator outlet ($\vartheta_{[6]}$)	NTC sensor	Od -50°C do +105°C	±0.3 °C @ 25°C ±1 °C @ 80°C ±1.2 °C @ -20°C
Temperature of R290 on controlling points ($\vartheta_{[1]}$, $\vartheta_{[2]}$, $\vartheta_{[3]}$, $\vartheta_{[4]}$)	Resistor - digital thermometer	Od -50°C do +110°C	±1°C with ±0.1°C of reading
Low pressure – evaporating pressure	Pressure transmitter	Od -1 bar do 12.8 bar	±1.2% of all measuring range
High pressure – condensation pressure	Pressure transmitter	Od 0 bar do 34.5 bar	±1.2% of all measuring range
Compressor frequency	Frequency regulator	Od 30 Hz do 65 Hz	3ph; 15.4 A and 7.5 kW output power and current
Unit running	EEV's microcontroller and DDC controller for unit regulation		

3.1 Test procedure and model validation

The water temperature at the evaporator inlet is the reference temperature of the cooling circuit, which is SET POINT of the chiller. The test was performed for a defined operating point "SET POINT", defined according to the water return temperature at the evaporator inlet of 14 °C, with a control range of ± 2 ° C. During the test, water was used to cool the condenser and as a heat source for the evaporator.

Table 6: Operating conditions during tests of the chiller

Variables	**Minimum**	**Maximum**
Compressor operating frequency, Hz	33	60
Water temperature at the evaporator inlet ("SET POINT"), °C	12.5	14.6
Volume flow of water through the evaporator, m^3/h	2.542	3.84
Water temperature at the condenser inlet, °C	34.7	39.8
Volume flow of water through the condenser, m^3/h	3.059	10.88
EEV openness, %	47	97

Measurements were collected for 10 steady-state chiller operating cases for different compressor operating frequencies. The real boundary conditions from the experimental tests were used as input data for the chiller operation simulation, which are listed in the table above, and called the boundary conditions.

The experimental compressor drive capacities are within 10% of the deviation from the results of the computer simulation of the reciprocating compressor model. The heat fluxes at the evaporator and condenser and the liquid cooler cooling factor are within ± 10% of the deviations at most, both can be seen in the following graphs.

EEV is programmed to maintain a superheat of 6°C, thus changing the valve opening as a function of the operating capacity of the compressor that generates the refrigerant mass flow. Satisfactory results within ± 10% deviation are obtained for different operating frequencies of the compressor compared to the simulation results of the EEV model.

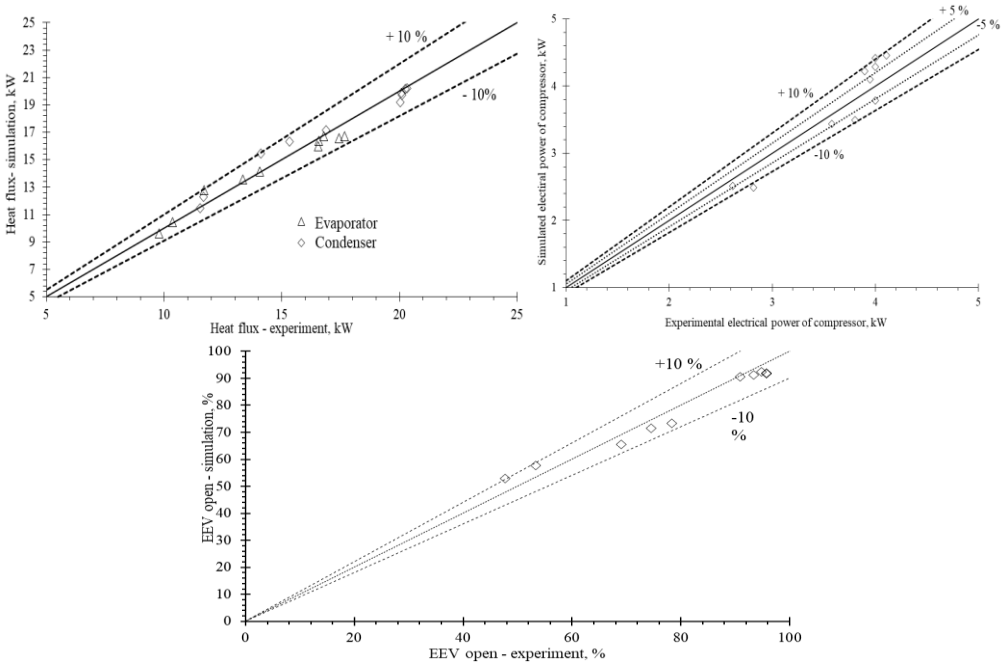

Figure 4: Results of mathematical model validation

4. SIMULATION RESULTS – REFRIGERANT CHARGE OPTIMIZATION

In this study, by using the simulation tool, the refrigerant charge is varied from 900 g to 1100 g for fixed compressor frequencies of 35 Hz, 50 Hz and 65 Hz, in one case; and in another frequencies are varied from 30 Hz up to 70 Hz for fixed refrigerant charge values of 900 g, 928 g and 956 g. The results are shown in Figure 5.

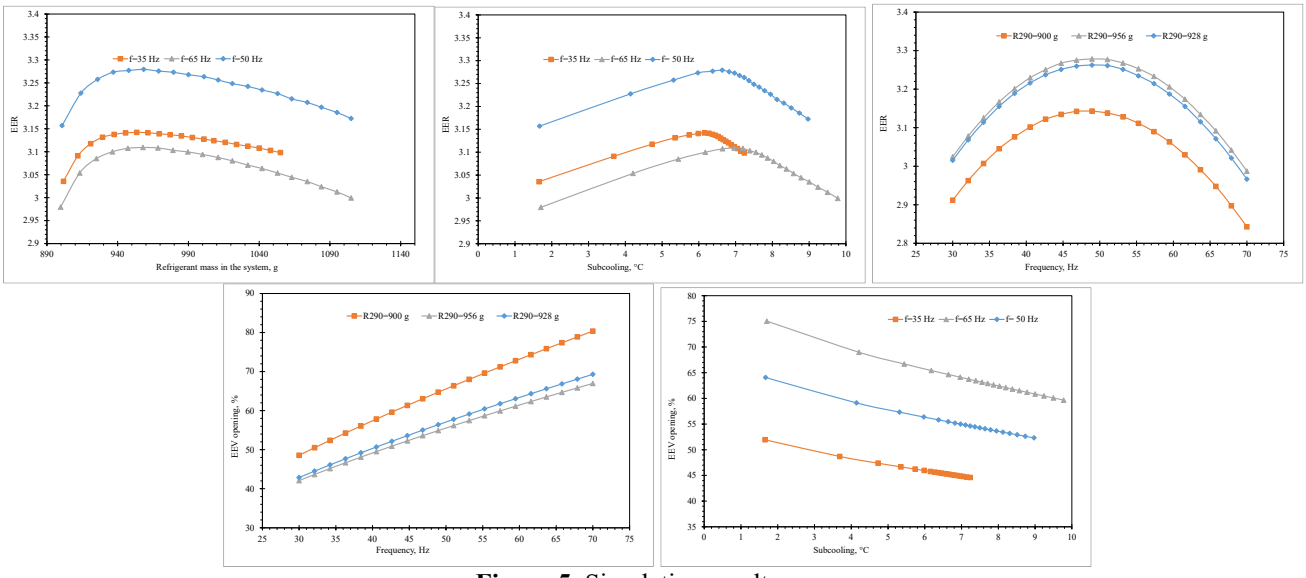

Figure 5: Simulation results

Results show that for a given compressor frequency value, the EER first increases with increasing values of the refrigerant charge up to a maximum value and then starts to decrease. For the three frequency values analyzed, the optimum charge was similar and around 960 g. Also, as the refrigerant charge increases so does the subcooling at the condenser outlet. The subcooling degree for the optimum charge was always between 6 and 7 °C.

For a given refrigerant charge value, it was observed that when the compressor frequency increases the EER first increases but then starts to decrease. The optimum frequency was around 50 Hz for the cases analyzed in this paper. As expected, the model predicts an increase of the EEV opening when increasing the compressor frequency. Also, when increasing the refrigerant charge, the condenser pressure increases and so does the pressure difference through the EEV, so the EEV opening should decrease as predicted by the model.

5. CONCLUSIONS

It can be said that the refrigerant charge is the crucial point in the design of a propane system (without liquid receiver) to obtain good working conditions. Model of the compressor and expansion valve helps to optimize the heat exchangers design or selection and also the system design. The following main conclusions are done with simulation in this work:

- best refrigerant charge for analyzed propane refrigeration unit system is 956 g;
- optimal subcooling degree is around 6.6°C;
- optimal working frequency is the 50 Hz - highest EER's;
- for optimal refrigerant charge of 956 g the EER's has the highest values;
- for optimal refrigerant charge of 956 g (highest amount of refrigerant) the EEV openings are the lowest;
- for optimal refrigerant charge of 956 g and optimal subcooling degrees (around 6,6°C) the discharge compressor temperatures are the lowest.

NOMENCLATURE

**All subscript numbers in angle brackets (e.g. [1]) in mathematical model follows same numbers at Figure 3.*
**In the nomenclature are included only main variables, rest of variables are covered in the paper.*

A	surface	m^2
c_p	Specific heat capacity	$J \cdot kg^{-1} \cdot K^{-1}$
d	diameter	m
h	Specific enthalpy	$J \cdot kg^{-1}$
$\dot{m}$	mass flow rate	$kg \cdot s^{-1}$
M	Mass	kg
$\dot{M}$	Mass flux	$kg \cdot s^{-1} \cdot m^{-2}$
n	Polytropic exponent	-
$\dot{N}_{rot}$	Number of rotations per time	s^{-1}
N	Number	-
p	Pressure	Pa
$\dot{Q}$	Heat flux	W
T	Temperature	K
$T_{cond,\Delta}$	is calculated condensation temperature influenced by increased refrigerant mass in the circuit	
V	Volume	m^3
V_0	Clearance volume	-
ε_0	Clearance factor	-
$\dot{V}$	Volume flow rate	$m^3 \cdot s^{-1}$
$\dot{W}$	Power	W
x	Quantity	$kg \cdot kg^{-1}$
ρ	Density (middle value with line on the top)	$kg \cdot m^{-3}$
$\varepsilon_{\dot{Q},ok}$	Heat transfer factor to the ambient	-
η	Efficiency	-
α	Heat transfer coefficient	$W \cdot m^{-2} \cdot K^{-1}$
λ	Heat conductivity	$W \cdot m^{-1} \cdot K^{-1}$
ϑ	Temperature	°C
Δ	Difference or loss	$J \cdot kg^{-1}$

Subscript

amb	ambient	cyl	cylender
ef	effective	cond	condenser/condensation
evap	evaporator/evaporation	rot	rotation

ref	refrigerant	in	indicated
vol	volumetric	hyd	hydraulic
sup	superheat	sub	subcooling

REFERENCES

American National Standards Institute (2007). ISA-75.01.01-2007 (60534-2-1 Mod): Flow Equations for Sizing Control Valves, *Research Triangle Park*, North Carolina 27709, USA: American National Standards Institute

Amalfi R. L. (2016). *Two-Phase Heat Transfer Mechanisms within Plate Heat Exchangers: Experiments, Modeling and Simulations*, Switzerland: École Polytechnique Fédérale de Lausanne (EPFL), THÈSE No 6856

Bauer F. (1988). Valve losses in reciprocating compressors. *International Compressor Enineering Conference at Purdue, West Lafayette, Purdue University*

Boeswirth L. and Milanova V. (1998) Simple but efficient methods for estimation of valve loss, capacity loss due to suction valve throttling and heat transfer cylinder *Internationl Compressor Engineering Conference at Purdue, Purdue University, West Lafayette, pp. 93-98*

Chuan Z., Shanwei M., Jiangpin C., and Zhijiu C. (2006.), Experimental analysis of R22 and R407c flow through electronic expansion valve, *Energy Conversion and Management 47, p. 529–544*

Cavallini A., Del Col D., Doretti L., Matkovic M., Rossetto L. and Zilio C. (2006) Condensation in horizontal smooth tubes: A new heat transfer model for heat exchanger design, *Heat Transfer Engineering 27 (8), pp. 31-38*

Collier J. and Thome J. (1996) *Convective boiling and condensation*, 3rd edition, New York: Oxford University Press

Hengel F., Heinz A. and Rieberer R. (2016) Performance analysis of a heat pump with desuperheater for residential buildings using different control and implementation strategies, *Applied Thermal Engineering, p. 256–265, 105*

Janković Z., Sieres Atienza J., Cerdeira-Perez F., Pavković B. (2018) Analysis of the impact of different operating conditions on the performance of a reversible heat pump with domestic hot water production, *International Journal of Refrigeration, 86*

Janković Z., Sieres J.A., Cerdeira F. P., Pavković B. (2016): *Steady-State Numerical Simulation of a Vapor Compression Heat Pump System as an Effective Method to Predict its Performance*, International Refrigeration and Air Conditioning Conference, Paper 1578

Li W. (2013) Simplified modeling analysis of mass flow characteristics in electronic expansion valve *Applied Thermal Engineering 53, pp. 8-12*

Qifang Y., Jiangping C. and Zhijiu C. (2007) Experimental investigation of R407C and R410A flow through electronic expansion valve *Energy Conversion and Management 48, pp. 1624-1630*

Longo G. A. i Gasparella A. (2007) HFC-410A vaporisation inside a commercial brazed plate heat exchanger *Experimental Thermal and Fluid Science (32), pp. 107-116*

Longo G. A. and Gasparella A. (2007) Heat transfer and pressure drop during HFC refrigerant vaporisation inside a brazed plate heat exchanger *International Journal of Heat and Mass Transfer 50 pp. 5194-5203*

Longo G. A. (2009) R410A condensation inside a commercial brazed plate heat exchanger *Experimental Thermal and Fluid Science 33, p. 284–291*

Nusselt W. (1919) Die Oberflachenkondensation des Wasserdampfes Zeit Ver. Deut. Ing (VDI) 60, pp. 541-575

Shah R. and Focke W. (1988) Plate Heat Exchanger and Their Design Theory *Heat Transfer Equipment Design, pp. 227-254*

Scarpa M., Emmi G. and Carli M. D. (2012) Validation of a numerical model aimed at the estimation of performance of vapor compression-based heat pumps *Energy and Buildings, p. 411–420, 47*

Thonon B. (1995) Design Method for Plate Evaporators and Condenser *1st International Conference on Process Intensification for the Chemical Industry, BHR Group Conference Series Publication, no. 18, pp. 37-47*

Vjacheslav N., Rozhentsev A. and Wang C.C. (2001) Rationally based model for evaluating the optimal refrigerant mass charge in refrigerating machines *Energy Conversion and Management no. 42, br. 18, pp. 2083-2095*

ACKNOWLEDGEMENT

This research was in part funded by University of Rijeka project (uniri-tehnic-18-14).

Thanks also go to the company Frigo Plus d.o.o. from Croatia, which manufactured, tested and provided this cooling unit to the end customer and disseminated information for research purposes.